The A245K Mutation Exposes Another Stage of the Bacterial L-Lactate Dehydrogenase Reaction Mechanism†

Paweł Kędzierski,*,‡ Kathleen Moreton,§ Antony R. Clarke,§ and J. John Holbrook§

Institute of Physical and Theoretical Chemistry, Wrocław University of Technology, 50-370 Wrocław, Poland, and Molecular Recognition Center and Department of Biochemistry, University of Bristol, Bristol, England

Received November 22, 2000; Revised Manuscript Received March 12, 2001

ABSTRACT: The A245K mutant of *Bacillus stearothermophilus* L-lactate dehydrogenase has been expressed in *Escherichia coli* and purified. A qualitative change in the reaction mechanism prior to the hydride transfer step in the reverse direction in the mutant is revealed. Both transient and steady state characteristics of the mutant are presented and show in contrast to the wild-type enzyme where a rearrangement of an enzyme−NADH−pyruvate complex is rate-limiting that in the mutant the rearrangement is much faster and hydride transfer is the first slow step. The steady state is limited by a new second slower conformation change involving an NAD^+ complex. The mutation may provide a valuable framework for inhibitor and drug design research.

Enzymes involved in main metabolic pathways have been the subject of extensive research, and their properties are relatively well-known, which promotes further investigation aimed at industrial or medical applications. On the other hand, details of reaction mechanisms of even frequently studied proteins such as lactate dehydrogenase (LDH,[1] EC 1.1.1.27, PDB entry 1LDN) are still not completely known.

In our study, we created a set of variants of *Bacillus stearothermophilus* LDH (*1*) (Figure 1) mutated at position 245 (position 246 in the PDB file). This place provides enough space for bulky side chains, therefore allowing well-defined changes in the proximity of the active site, while not disrupting the protein structure. The selected position 245 is occupied by an alanine residue in wild-type *B. stearothermophilus* LDH (BsLDH) or by the much bigger tyrosine in some other highly homologous LDHs (occurring, for example, in mammals). The side chains of both alanine and tyrosine residues at position 245 are stretched inside a cleft on the protein surface (Figure 1).

One of the mutations (Ala245 → Lys) resulted in a qualitative change in the reaction mechanism, exposing two stages (one novel) in the transient kinetics. The kinetic properties of the mutant protein were compared to the native protein behavior under different conditions. The comparison of the kinetic effects of isotope substitution and of different solvent viscosities leads to the identification of the newly exposed reaction stage as the hydride transfer. A plausible explanation of the change in the reaction mechanism is also proposed.

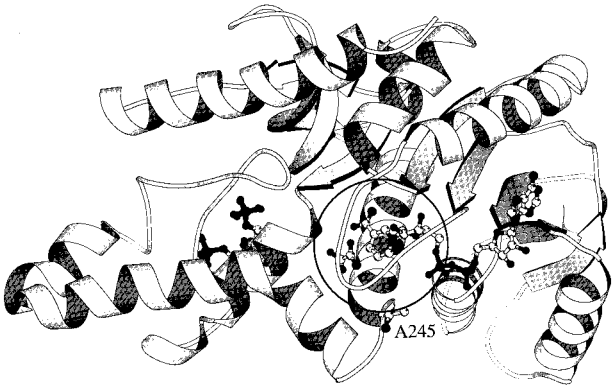

FIGURE 1: Ribbon drawing of one subunit of *B. stearothermophilus* L-lactate dehydrogenase. The interface of the subunits in a dimer is on the bottom side of this picture, and the interface of two dimers forming a tetramer is on the back side. NADH, pyruvate, and the alanine moiety at the mutated position 245 are presented as ball-and-stick models. The active site is marked with a circle.

MATERIALS AND METHODS

The wild-type gene of *B. stearothermophilus* (NCA1503 strain) L-lactate dehydrogenase (LDH, EC 1.1.1.27) was first cloned, sequenced, and expressed by Barstow et al. (*2*). This gene, cloned in the pKK223-3 (Pharmacia LKB Biotechnology, Milton Keynes, U.K.) expression vector, provided the template for generating two limited libraries of mutants using overlap-extension polymerase chain reaction (*3*, *4*). The primer oligonucleotides were synthesized using a Du Pont Coder 300 DNA synthesizer. The two flanking primers, used for incorporation into the pKK223 plasmid, were GGGATC-

† P.K. acknowledges the Poznań Supercomputing Center and the Wrocław Supercomputing and Networking Center where some of the computer modeling was performed, and the support from the European Community TEMPUS fellowship and from Wrocław University of Technology. J.J.H. and A.R.C. thank the BBSRC for project grant support and for use of the Molecular Recognition Centre facilities.

* To whom correspondence should be addressed. Phone: +48 (71) 320 32 00. Fax: +48 (71) 320 33 64. E-mail: P.Kedzierski@mml.ch.pwr.wroc.pl.

‡ Wroclaw University of Technology.

§ Molecular Recognition Center and Department of Biochemistry, University of Bristol, England.

[1] Abbreviations: NADH and NAD^+, nicotinamide adenine dinucleotide, in reduced and oxidized forms, respectively; LDH, lactate dehydrogenase; BsLDH, *B. stearothermophilus* LDH; A245K, Ala245 → Lys mutant of BsLDH; FBP, fructose 1,6-bisphosphate; PCR, polymerase chain reaction; TEA, triethylamine.

10.1021/bi0026775 CCC: $20.00
Published on Web 05/24/2001

CGTCGACCTGCAGC and AGCGGATAACAATTTCACAC, respectively. We used two different sets of mutating oligonucleotides, namely, GAGAAAAAAGGANTNACGTACTACGGG and GAGAAAAAAGGAXAGACGTACTACGGG with their respective complements, where N denotes any base and X is C, A, or G. The varied codons are underlined.

The PCR was performed in 50 μL aliquots containing 30 ng of template DNA, 50 mM KCl, 10 mM Tris (pH 8.3), 1.5 mM $MgCl_2$, 0.01% (w/v) gelatine, dNTPs (200 mM each), primers (0.5−1 mM each), and 2.5 units of Taq DNA polymerase (Boehringer Mannheim Ltd.). Each reaction mixture was subjected to 20 cycles of PCR (1 min at 94 °C, 1 min at 50 °C, 2 min at 72 °C, and 15 min at 72 °C at the end of the program) in a Perkin-Elmer thermal cycler. The overlapping halves of the LDH gene were separated from contaminants on low-melting point agarose from Sigma, purified using the SephaGlas DNA purification kit (Pharmacia LKB), and then underwent seven cycles of annealing and overlap extension without addition of primers in the thermal cycle as described above. The full-length gene was amplified with flanking primers over 25 cycles under the same conditions, isolated on agarose, and completed with a final step of 15 min at 72 °C.

The produced DNA was finally purified using the same method that was used before, cut with *Eco*RI and *Pst*I (in OnePhorAll 1× buffer, Pharmacia LKB, for 90 min at 37 °C), and ligated into 0.5 μg of pKK223 DNA using T4 ligase (United States Biochemicals).

Transformation of Escherichia coli and Screening for Mutants. The solution of the plasmid was used to transform *E. coli* TG2 cells (*lac-pro, supE, thi, hsd*D5, [F′*tra*D36, *pro*AB, *lac*I^Q, *lac*Z ΔM15]). After overnight incubation in 2× YT broth medium (2% tryptone, 2% yeast extract, and 1% NaCl) with 100 μg/mL ampicillin, several clones were picked up and used to inoculate an array of 5 mL cultures in the same medium. After being grown for 2 days, crude LDH extracts were used for preliminary identification of mutant proteins by means of an activity assay. Since the DNA encoding LDH carries also its own promoter sequences from *B. stearothermophilus*, which are very active in *E. coli*, the transformants constitutively produce up to 35% of the total cellular protein of soluble LDH (*2*).

Thanks to the temperature resistance of the *B. stearothermophilus* protein, it could be harvested by thermal denaturation of sonicated cell extracts (for 30 min at 68 °C) and subsequent removal of the solid debris. The plasmid DNA from selected clones was harvested from 100 mL cultures using the QIAGEN Tip-100 kit and identified using either a Du Pont Genesis 2000 automatic sequencer, or manually, using the Sequenase 2.0 sequencing kit from United States Biochemicals. We identified six mutants: A245F (TTT codon), A245L (CTA codon), A245M (ATG codon), A245K (AAG codon), A245Q (CAG codon), and A245E (GAG codon). Clones of the A245F, A245M, A245K, A245Q, and A245E strains were used for preparative-scale mutant expression.

Protein Preparation and Purification. Cells harvested from 2 L of 48−72 h old cultures were suspended in a minimal volume of 50 mM TEA buffer (pH 7.5) and sonicated, and the native *E. coli* proteins were denaturated for 30 min at 68 °C. Solid debris was discarded by centrifugation, and the resulting solution of LDH was purified on a Q-Sepharose column (Pharmacia LKB) connected to an NaCl gradient in buffer containing azide.

The purity of the LDH protein after chromatography was checked by means of SDS−PAGE, revealing that the preparations were contaminated by no more than 2% of other proteins (as judged from Comassie Blue staining). Therefore, they were used in all kinetic measurements without further purification. In some cases, further purification was necessary, and it was carried out on a Blue Sepharose affinity column connected to a 0 to 2 M salt gradient in 50 mM TEA buffer (pH 7.0). The purified enzyme solutions were immediately precipitated with solid ammonium sulfate [0.43 g of $(NH_4)_2SO_4$/mL of the solution] and stored at 4 °C.

Kinetics Measurements. The protein solution for the measurements consisted of the ammonium sulfate precipitate dissolved in a small volume of buffer and dialyzed overnight. For kinetics measurements, 20 mM Bis-Tris (pH 6.0) with 50 mM KCl buffer was used, as it proved to be optimal for the reaction performed by *B. stearothermophilus* LDH. Concentrations of proteins in freshly dialyzed solutions were evaluated by means of their absorbance at 280 nm using the absorbance coefficient of 0.91 mg cm^{-1} mL^{-1}.

The transient kinetics was measured by rapid mixing of two equal volumes of protein and substrate solutions. The stopped-flow apparatus had a dead time of 2 ms, and it was equipped with a 2 mm quartz cuvette. For single-turnover conditions, the protein solution (A) contained 100 μM NADH or NADD and 100 μM enzyme (active centers), which corresponds to 50 μM in the reaction cuvette. For steady state conditions, the enzyme concentration was ∼1−5 μM (adjusted experimentally). The substrate solutions (B) were prepared for a range of pyruvate concentrations from 0.05 to 100 mM. The reaction was always performed in 20 mM Bis-Tris (pH 6.0) containing 5 mM fructose 1,6-bisphosphate and 50 mM KCl. For the evaluation of the influence of the reversed order of substrate binding on the kinetic parameters, we performed the measurements under single-turnover conditions using (A) a solution of 100 μM enzyme with pyruvate and (B) a solution containing 100 μM NADH or NADD. The other conditions were kept identical for comparison. High-viscosity media used to evaluate the effect of solution viscosity on reaction rate contained also 40% (v/v) glycerol. All the measurements were taken at 25.0 ± 0.1 °C. NADH (Boehringer Mannheim) and FBP (Sigma) were second-grade (98% pure). A-side NADD, necessary for evaluation of primary isotopic effects, was synthesized by a method of Cleland et al. (*5*), from perdeuterioethanol (99% D) and NAD^+ (98% grade), in 20 mM Tris buffer (pH 8.5). The NADD solution was purified from contaminating horse liver alcohol dehydrogenase and yeast aldehyde dehydrogenase used in its synthesis either by several extractions with CCl_4 or by ultrafiltration. The final solution was divided into small aliquots and stored frozen at −20 °C for up to 4 weeks. All solutions for kinetic measurements were prepared from stocks or dry preparations and used on the same day. Concentrations of NADH and NADD were judged from the absorbance at 340 nm using a molar coefficient of 6220 M^{-1} cm^{-1}.

The record of NADH absorbance at 340 nm over 0.1 s was filtered from high-frequency fluctuations using a 200 μs filter. One thousand data points were collected each time, but 20 initial points were discarded. Each reaction was repeated at least five times, and the average results were analyzed. Data for steady state conditions were collected within the range of 100−80% of the initial absorbance and subjected to linear regression analysis. The resulting slope was recalculated to the reaction rate V([S]) defined as the turnover of one active center (moles of pyruvate per second), and the kinetic parameters k_{cat}, K_M, and K_i were calculated numerically by fitting of experimental data to the extended Michaelis−Menten model with substrate inhibition [$(k_{cat}[S])/([S] + [S]/K_M)$] using GraFit 3.0 (Erithacus Software Ltd., Staines, U.K.). Data for single-turnover conditions were collected in the same way and fitted with a single-exponential function. In the case of mutant A245K, the single-turnover data did not fit to a single-exponential curve and were well approximated with a double-exponential function. These results reveal a qualitative change in the reaction mechanism and are discussed further in this paper.

Computer Modeling. The structure of *B. stearotermophilus* lactate dehydrogenase complexed with the allosteric activator (FBP), NADH, and a substrate analogue (oxamate) was determined by Wigley et al. using X-ray crystallography (*1*). The original Protein Data Bank file was processed using the Insight II molecular modeling package (*6*). Because BsLDH exists in solution as an equilibrium of dimer and tetramer forms (however, shifted to tetramers), only a dimer was used for modeling. This has a negligible effect on protein activity (*7*). A pyruvate molecule was built within the active center by substitution of the oxamate NH_2 group with a CH_3 group. The activator molecules (FBP) were removed as well, because their role is negligible for dimers (*8*). Hydrogen atoms were added as for pH 7.0 using the Biopolymer module of Insight II. The state of protonation was adjusted manually wherever experimental data were available (*9*−*11*); it applied to Asp143 (neutral), His188 (+), His195 (+), Glu197 (neutral), and C-terminal Thr330 (COO^-). The supermolecule consisting of the enzyme, pyruvate, NADH, and crystalline water molecules was covered with a 5 Å layer of water. Potential functions and partial charges on all atoms were set using the CVFF force field (*12*), which is a well-tested class I force field used in Discover versions 2.9 and 3.1. The system was therefore subject to extensive energy minimization, to the final maximal energy derivative of 0.001 kcal/mol.

The optimized system was used to create mutant supermolecules. The Ala245 residue (residue 246 in the PDB file) was changed to methionine, phenylalanine, lysine, glutamine, and glutamate using the Biopolymer module of Insight II. All mutant structures underwent a second optimization afterward.

The scan of the conformational space was carried out using molecular dynamics calculations. Due to the high computational cost, only a 20 Å sphere of bulk water around the mutant residue was retained in these calculations, and all the residues further than 15 Å from the substrate were kept frozen. All the systems were first equilibrated over 200 fs to achieve a temperature of 300 K. Afterward, they underwent 30 ps of dynamics. The conformation of the system was saved every 200 fs.

Table 1: Kinetic Rate Constant Measurements for a Set of Mutants of *B. stearothermophilus* LDH[a]

	single turnover		steady state	
	k_{cat} (s^{-1})	exptl error	k_{cat} (s^{-1})	exptl error
A245F	240	±30	120	±7
A245M	330	±40	142	±7
A245Q	400	±40	167	±8
A245E	170	±30	49	±5
A245K	730	±70	76	±5
	67	±5		
wild type	450	±45	190	±10

[a] The conditions were as follows: 5 mM FBP, 50 μM enzyme (subunits), 50 μM NADH, Bis-Tris (pH 6.0), and 50 mM KCl at 25.0 °C (see Materials and Methods).

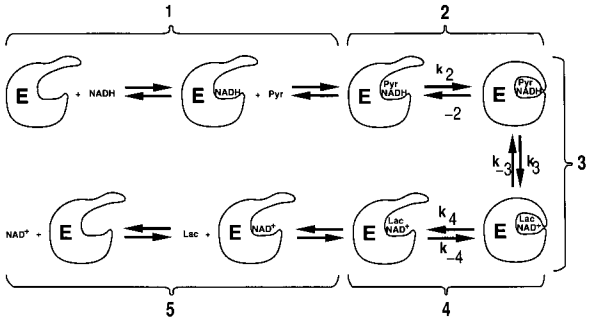

FIGURE 2: General mechanism of lactate dehydrogenase action: (1) substrate binding, (2) conformational activation (closing of the active site), (3) pyruvate reduction, (4) conformational deactivation, and (5) release of products.

RESULTS AND DISCUSSION

Measured reaction rate constants for both steady state and transient conditions are listed in Table 1.

One can observe that the maximal rate of the enzyme is different when measured over multiple turnovers of the substrate than when the enzyme performs just one reaction cycle. This effect is easy to explain on basis of the general mechanism of the reaction performed by lactate dehydrogenases (Figure 2). The whole reaction goes through many stages: substrate binding, conformational activation (*13*, *14*), and then pyruvate reduction, followed by reverse conformational change and products dissociation. The conformational change is related to a movement of a flexible loop (residues 99−110) from the solvent to close over the active site. As shown by Waldman et al. (*15*) and Dunn et al. (*16*), closing of the loop that enforces isolation of the active center from bulk solvent is necessary for the reaction to proceed with a noticeable rate. Since our observation is based on changes in the NADH specific absorbance at 340 nm, the rate, which we observe at the first turnover, must be either the explicit rate of NADH oxidation or the rate of one of the steps prior to oxidation (if slower). In practice, this is probably the loop movement since binding of substrates is controlled by diffusion, which is a few orders of magnitude faster. On the other hand, the second and subsequent turnovers cannot be performed unless the enzyme has completed further stages of the first turnover of the reaction. This may lead to a conclusion that the rate with multiple turnovers is limited by one of the stages following NADH oxidation which is the slowest one over the whole cycle. It was discussed by Holbrook and Gutfreund (*17*), who also pointed out that under steady state conditions some fraction

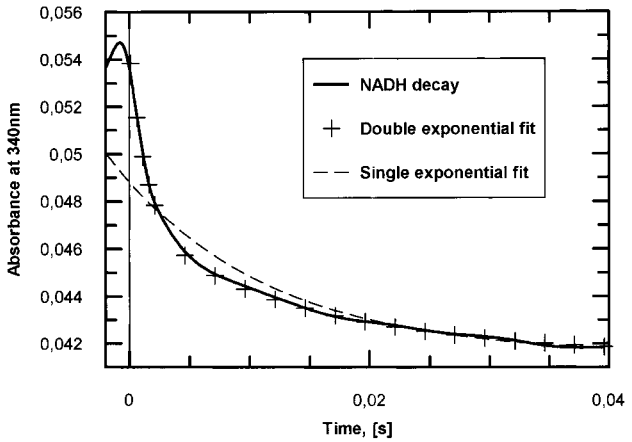

FIGURE 3: Transient kinetics of the BsLDH A245K mutant enzyme. The double-exponential character of the curve of NADH turnover reveals the two-stage nature of the process.

Table 2: Primary Isotopic Effects on the Reaction Performed by a Set of BsLDH Mutants[a]

	single-turnover primary isotopic effect
A245F	1.0 ± 0.1 (none)
A245M	1.0 ± 0.1 (none)
A245K	2.0 ± 0.3 for the first fast phase
	1.0 ± 0.2 for the second phase
A245Q	1.0 ± 0.1 (none)
A245E	1.0 ± 0.1 (none)
wild type	1.0 ± 0.1 (none)

[a] Conditions are described in the Table 1 footnote.

of the catalyst molecules is bound in form of a dead-end complex enzyme (NAD^+, pyruvate) which explains substrate inhibition of LDHs.

Some explanation of why two different values of the catalytic constant for A245K are observed is necessary. The trace of changes in absorbance at 340 nm over time during a single turnover performed by BsLDH A245K is presented in Figure 3. It was fitted with both a single-exponential and a double-exponential function. It is clear that these data are much better fitted using a double-exponential function which strongly suggest a two-stage nature of the reaction. The origin of this effect will be discussed later.

Compared to Figure 2, the rate visible in single-turnover measurements may be either the rate of NADH oxidation or the rate of closing of the active center. To distinguish which is the slower step for each of the mutants, measurements of the primary isotopic effect were performed (Table 2). The experimental error for these results is ~10%. They show clearly that the reaction, in which the rate is limited by hydride transfer, is the first stage of the process performed by the A245K mutant. The observed isotopic effect of 2.0 is however smaller that one could expect; it may be explained that the rate of NADD oxidation becomes limited by another phase of the mechanism (Figure 2), which does not show the isotopic effect. Another explanation is that the highest isotopic effect is observed only when atoms of the donor, the acceptor, and the transferred hydride are collinear. However, theoretical studies on transition state structures for dehydrogenases (*18*−*21*), although not conclusive, suggest that this is not the case here.

In summary, we conclude that the first observable phase in A245K catalysis is hydride transfer. It is not obvious which

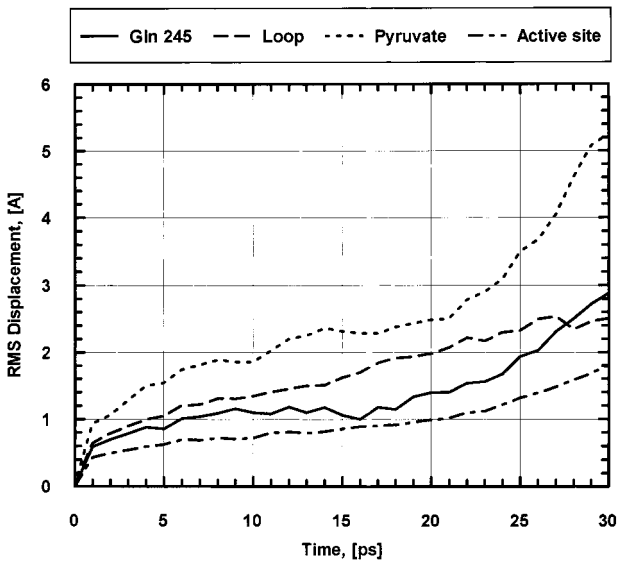

FIGURE 4: Mobility within the active site of the BsLDH A245Q mutant over 30 ps of molecular dynamics. The curve denoted "Active site" concers residues which have at least one atom within 3.0 Å of pyruvate; the curve denoted "Loop" concerns residues from Ala100 to Leu112.

stage shown in Figure 2 is responsible for the slower second phase of NADH decay. However, since we observe that some NADH is still present (absorbance at 340 nm), we can draw a conclusion that the fast reaction of NADH oxidation does not lead to immediate and complete conversion of all the NADH and that the ratio of NADH to NAD^+ complexes on enzyme is 1:2. Instead, the reaction reaches a state close to equilibrium between NAD^+ and a significant fraction of unprocessed NADH. Interestingly, these measurements may allow one to estimate the extent of stabilization of products or destabilization of substrates bound to the enzyme by means of the equilibrium ratio of NADH and NAD^+ in comparison to solution. Afterward, draining of NAD^+ through subsequent reaction steps leads to a slow decay of this residual NADH and to disappearance of absorbance at 340 nm.

The interesting point is what happens with the flexible loop, in which movement is believed to limit the turnover rate of the native enzyme and all the other mutants. The first idea we tested was that it could have been kept in an open conformation over the whole reaction cycle. It might arise due to repulsion of introduced positive charge at position 245 and positively charged side chains in the loop, the most important of which is arginine 109 (*22*). This question was addressed by computer modeling. However, not sufficiently accurate for quantitative measurements, computer modeling represents well qualitative features of relatively strong and long-range electrostatic interactions, and therefore, it should show if either loop-up or loop-down is the preferred state of our mutant. Geometry optimization, as described in Materials and Methods, did not result in loop-up structure for any of our mutants. Molecular dynamics modeling over 30 ps suggests that the loop-down structure is more stable for A245K than for the native enzyme, since the amplitudes of vibrations within the active site are smaller and the frequency seems to be larger in A245K than in the wild-type structure. Figures 4 and 5 compare active site mobility of mutants A245Q and A245K. Fluctuations of wild-type structure are

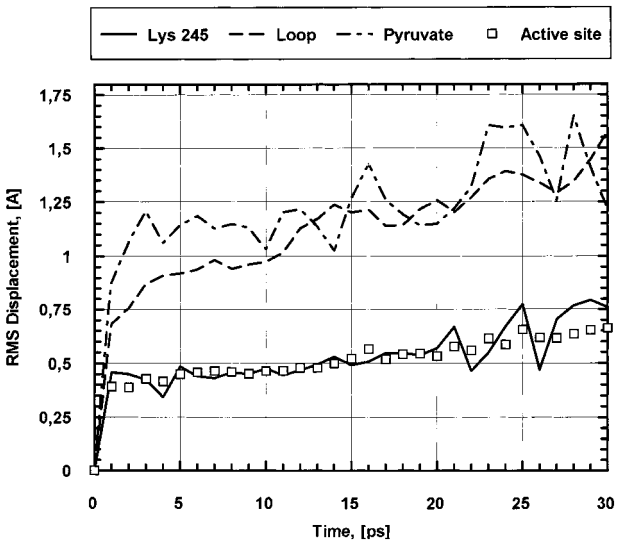

FIGURE 5: Mobility within the active site of the BsLDH A245K mutant. The relatively small amplitude of vibrations and their frequency show unusual rigidity within the active site of this mutant. Descriptions of the curves are the same as in the legend of Figure 4.

similar to those exhibited by A245Q, but the latter is directly comparable with the A245K mutant since glutamine and lysine are sterically similar and our molecular dynamics results show they both form a hydrogen bond to the phosphoric group of the NADH cofactor.

If the loop is not fixed in the open position, other explanations are that either it closes faster in mutant or the movement is somehow limited or impaired, and therefore, the enzyme works with a half-open active site. We tried to measure explicitly the rate of loop closure by means of tryptophan fluorescence studies on a mutant with a single tryptophan residue in position 106 in the loop and with the A245K mutation (*13*). However, the mutant protein was too unstable to isolate in a pure form. We used an alternative method to evaluate the mechanistic effect of the A245K mutation (*16*). Reaction media containing 40% (w/w) glycerol make enzymes limited by loop movement slower by a factor of 4−5. The A245K enzyme is twice as fast (at the first visible stage of transient kinetics) than wild-type LDH, and therefore, the viscous reaction buffer should limit the first visible rate if movement of the loop is not faster by 1 order of magnitude than in the wild type. What we observe is that the first stage is not affected by the high-viscosity medium, whereas the second visible stage slows significantly (Table 3). On the other hand, the effect of viscous medium is similar for both enzymes under steady state conditions (Figure 6).

Another interesting effect was observed when the order of substrate binding was reversed; the first stage of reaction performed by A245K LDH slowed, showing that binding of the large NADH molecule becomes the limiting step. This effect is absent for the wild type. A plausible reason is a higher energetic barrier of NADH binding, presumably because of the limited flexibility of the loop that closes the active site with the nicotinamide ring of NADH. Binding of a small molecule of pyruvate is not impaired since it can easily diffuse even through the loop (Figure 1). This explanation assumes that A245K obeys an ordered reaction mechanism as suggested in Figure 2, i.e., that the enzyme−

Table 3: Transient Kinetics Characteristics of Wild-Type BsLDH and the A245K Mutant in Relation to the Viscosity of Reaction Media and Order of Substrate Binding[a]

	normal viscosity		with 40% glycerol	
conditions	rate 1 (s^{-1})	rate 2 (s^{-1})	rate 1 (s^{-1})	rate 2 (s^{-1})
NADH on A245K, with pyruvate	726 ± 75	68 ± 5	740 ± 75	16 ± 3
NADD on A245K, with pyruvate	425 ± 45	67 ± 5	477 ± 50	23 ± 3
NADH on WT, with pyruvate	450 ± 45		118 ± 12	
NADD on WT, with pyruvate	444 ± 45		122 ± 12	
pyruvate on A245K, with NADH	507 ± 50	64 ± 5	362 ± 35	25 ± 3
pyruvate on A245K, with NADD	295 ± 30	60 ± 4	276 ± 30	27 ± 3
pyruvate on WT, with NADH	419 ± 45		121 ± 12	
pyruvate on WT, with NADD	379 ± 40		115 ± 11	

[a] The conditions are described in the Table 1 footnote. For A245K, the second reaction phase seems to correspond to the behavior of the wild-type enzyme. The first phase of the reaction assessed for A245K should be hydride transfer.

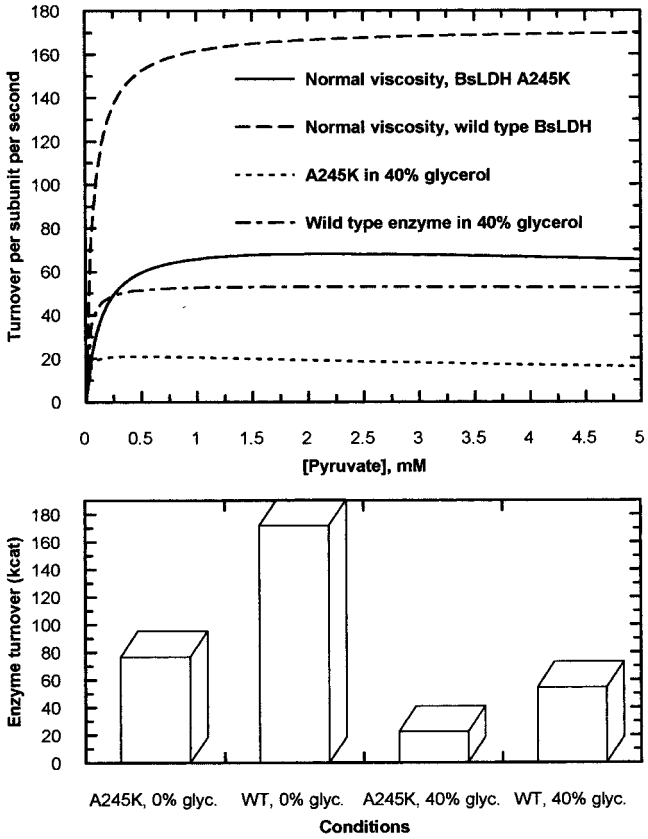

FIGURE 6: Effect of medium viscosity on the reaction rate under steady state conditions of BsLDH: the wild type and the A245K mutant. Both the wild type and the A245K mutant are similarly susceptible to the influence of buffer viscosity on reaction rate under steady state conditions.

NADH complex is formed first. This was confirmed for the wild-type enzyme (*23*), and it is unlikely to be different for A245K. The effects of the order of substrate binding on enzyme function for the wild type and the A245K mutant are compared in Table 3.

CONCLUSIONS

The appearance of two distinct stages in the transient kinetics of the BsLDH A245K mutant may be explained if we assume that not the first stage, but the third or fourth one, is the limiting step in the general reaction mechanism

(Figure 2). In that case, the first observable rate would be the relatively fast process of NADH oxidation, leading to on-enzyme equilibrium between NADH and NAD^+. Subsequent draining of NAD^+ through the further stages of the reaction will then result in slow decay of the remaining NADH. The measurements of single-turnover first-stage rates of the BsLDH A245K mutant in media of low and high viscosity show no effect of viscosity on the reaction rate, whereas the native enzyme works much slower in a viscous solution. Similarly, the primary isotopic effect on hydride transfer is ~2 for the mutated protein and 1 for the wild type. Both observations support the conclusion that for native BsLDH the slower stage consists of a conformational change and for the A245K mutant it is hydride transfer, independent of the viscosity of the reaction buffer. The second visible stage in transient kinetics of A245K has characteristics similar to those of the wild type. It slows significantly in viscous buffer, and it does not show isotopic effect; therefore, this must be also controlled by the rate of conformational change. Moreover, this second rate of A245K is similar to the rate under steady state conditions, indicating that it might be controlled by the same kinetic bottleneck stage, the slowest one over the whole reaction cycle.

The main change in enzyme function triggered by the mutation of Ala245 to lysine is concerned with the movement of a flexible loop covering the active site of the enzyme. In this study, we address the question of why the loop movement is no longer observed: does it become faster, or is it somehow impaired and the reaction runs with a half-opened active site. Since the viscosity of 40% glycerol does not return the kinetics of the mutant to a single exponential (which one could expect if loop movement became slower than NADH oxidation), we tried to exchange the order of substrate binding. The wild-type enzyme turnover rate does not depend on the order of substrate addition. If the conformational change was faster in the mutant, we would expect no effect. However, this is not the case. When NADH is bound to A245K after pyruvate, the first step of the reaction becomes slower but is still independent of buffer viscosity, and the kinetic isotopic effect is lowered toward 1. A reasonable explanation is that in the case of mutant protein movement of the loop covering the active site is limited and the conformation of the loop is more rigid than in the wild-type enzyme. Binding of a small pyruvate molecule is not impaired, but binding of NADH requires overcoming a higher energetic barrier. This explanation is also supported by computer modeling, since the A245K mutant exhibits unusual rigidity of the conformation of the active site over 30 ps of molecular dynamics. A likely reason for this rigidity might be the existence of a strong salt bridge between the Lys245 NH_3^+ group and the pyrophosphate part of the NADH molecule.

REFERENCES

1. Wigley, D. B., Gamblin, S. T., Turkenburg, J. P., Dodson, E. J., Piontek, K., Muirhead, H., and Holbrook, J. J. (1992) *J. Mol. Biol. 223*, 317−335.
2. Barstow, D. A., Clarke, A. R., Chia, W. N., Wigley, D., Sharman, A. F., Holbrook, J. J., Atkinson, T., and Minton, N.P. (1986) *Gene 46*, 47−55.
3. Ho, S. N., Hunt, H. D., Horton, R. M., Pullen, J. K., and Pease, L. R. (1988) *Gene 77*, 51−59.
4. Reikofski, J., and Tao, B. Y. (1992) *Biotechnol. Adv. 10* (4), 535−547.
5. Viola, R. E., Cook, P. F., and Cleland, W. W. (1979) *Anal. Biochem. 96*, 334−340.
6. Biosym Technologies Inc. (1993) *Insight II* and *Discover*, version 2.9, San Diego.
7. Jackson, R. M., Gelpi, J. L., Cortes, A., Emery, D. C., Wilks, H. M., Morethon, K. M., Halsall, D. J., Sleigh, R. N., Behan-Martin, M., Jones, G. R., Clarke, A. R., and Holbrook, J. J. (1992) *Biochemistry 31*, 8307−8314.
8. Iwata, S., and Ohta, T. (1993) *J. Mol. Biol. 230*, 21−27.
9. Wilks, H. M., Hart, K. W., Feeney, R., Dunn, C. R., Muirhead, H., Chia, W. N., Barstow, D. A., Atkinson, T., Clarke, A. R., and Holbrook, J. J. (1988) *Science 242*, 1541−1544.
10. Cortes, A., Emery, D. C., Halsall, D. J., Jackson, R. M., Clarke, A. R., and Holbrook, J. J. (1992) *Protein Sci. 1*, 892−901.
11. Nobbs, T. J., Cortes, A., Gelpi, J. L., Holbrook, J. J., Atkinson, T., Scaven, M. D., and Nicholls, D. J. (1994) *Biochem. J. 300*, 491−499.
12. Biosym Technologies Inc. (1993) *Discover version 2.9/3.1 User Guide*, Part 1, Chapter 3, San Diego.
13. Atkinson, T., Barstow, D. A., Chia, W. N., Clarke, A. R., Hart, K. W., Waldman, A. D. B., Wigley, D. B., Wilks, H., and Holbrook, J. J. (1987) *Biochem. Soc. Trans. 15*, 991−993.
14. Kotik, M., and Zuber, H. (1992) *Biochemistry 31*, 7787−7795.
15. Waldman, A. D. B., Hart, K. W., Clarke, A. R., Wigley, D. B., Barstow, D. A., Atkinson, T., Chia, W. N., and Holbrook, J. J. (1988) *Biochem. Biophys. Res. Commun. 150*, 752−759.
16. Dunn, C. R., Wilks, H. M., Halsall, D. J., Atkinson, T., Clarke, A. R., Muirhead, H., and Holbrook, J. J. (1991) *Philos. Trans. R. Soc. London, Ser. B 332*, 177−184.
17. Holbrook, J. J., and Gutfreund, H. (1973) *FEBS Lett. 31* (2), 157−169.
18. Andres, J., Moliner, V., Krechl, J., and Silla, E. (1993) *Bioorg. Chem. 21*, 260−274.
19. Ranganathan, S., and Gready, J. E. (1994) *J. Chem. Soc., Faraday Trans. 90* (14), 2047−2056.
20. Andres, J., Moliner, V., Krechl, J., and Silla, E. (1995) *J. Chem. Soc., Perkin Trans. 2 7*, 1551−1558.
21. Ranganathan, S., and Gready, J. E. (1997) *J. Phys. Chem. B 101* (28), 5614−5618.
22. Clarke, A. R., Wigley, D. B., Chia, W. N., Barstow, D., Atkinson, T., and Holbrook, J. J. (1986) *Nature 324*, 699−702.
23. Takenaka, Y., and Schwert, G. (1956) *J. Biol. Chem. 223*, 157−170.

BI0026775